EUROPEAN ORGANIZATION FOR NUCLEAR RESEARCH

CERN-EP-2000-113
18 August, 2000

Measurement of W boson polarisations and CP-violating triple gauge couplings from W^+W^- production at LEP

The OPAL Collaboration

Abstract

Measurements are presented of the polarisation of W^+W^- boson pairs produced in e^+e^- collisions, and of CP-violating WWZ and WWγ trilinear gauge couplings. The data were recorded by the OPAL experiment at LEP during 1998, where a total integrated luminosity of 183 pb^{-1} was obtained at a centre-of-mass energy of 189 GeV. The measurements are performed through a spin density matrix analysis of the W boson decay products. The fraction of W bosons produced with longitudinal polarisation was found to be $\sigma_L/\sigma_{total} = (21.0 \pm 3.3 \pm 1.6)\%$ where the first error is statistical and the second systematic. The joint W boson pair production fractions were found to be $\sigma_{TT}/\sigma_{total} = (78.1 \pm 9.0 \pm 3.2)\%$, $\sigma_{LL}/\sigma_{total} = (20.1 \pm 7.2 \pm 1.8)\%$ and $\sigma_{TL}/\sigma_{total} = (1.8 \pm 14.7 \pm 3.8)\%$. In the CP-violating trilinear gauge coupling sector we find $\tilde{\kappa}_z = -0.20^{+0.10}_{-0.07}$, $g_4^z = -0.02^{+0.32}_{-0.33}$ and $\tilde{\lambda}_z = -0.18^{+0.24}_{-0.16}$, where errors include both statistical and systematic uncertainties. In each case the coupling is determined with all other couplings set to their Standard Model values except those related to the measured coupling via $SU(2)_L \times U(1)_Y$ symmetry. These results are consistent with Standard Model expectations.

(To be submitted to Eur. Phys. J. C)

The OPAL Collaboration

G. Abbiendi[2], K. Ackerstaff[8], C. Ainsley[5], P.F. Åkesson[3], G. Alexander[22], J. Allison[16], K.J. Anderson[9], S. Arcelli[17], S. Asai[23], S.F. Ashby[1], D. Axen[27], G. Azuelos[18,a], I. Bailey[26], A.H. Ball[8], E. Barberio[8], R.J. Barlow[16], S. Baumann[3], T. Behnke[25], K.W. Bell[20], G. Bella[22], A. Bellerive[9], G. Benelli[2], S. Bentvelsen[8], S. Bethke[32], O. Biebel[32], I.J. Bloodworth[1], O. Boeriu[10], P. Bock[11], J. Böhme[14,h], D. Bonacorsi[2], M. Boutemeur[31], S. Braibant[8], P. Bright-Thomas[1], L. Brigliadori[2], R.M. Brown[20], H.J. Burckhart[8], J. Cammin[3], P. Capiluppi[2], R.K. Carnegie[6], A.A. Carter[13], J.R. Carter[5], C.Y. Chang[17], D.G. Charlton[1,b], P.E.L. Clarke[15], E. Clay[15], I. Cohen[22], O.C. Cooke[8], J. Couchman[15], C. Couyoumtzelis[13], R.L. Coxe[9], A. Csilling[15,j], M. Cuffiani[2], S. Dado[21], G.M. Dallavalle[2], S. Dallison[16], A. de Roeck[8], E. de Wolf[8], P. Dervan[15], K. Desch[25], B. Dienes[30,h], M.S. Dixit[7], M. Donkers[6], J. Dubbert[31], E. Duchovni[24], G. Duckeck[31], I.P. Duerdoth[16], P.G. Estabrooks[6], E. Etzion[22], F. Fabbri[2], M. Fanti[2], L. Feld[10], P. Ferrari[12], F. Fiedler[8], I. Fleck[10], M. Ford[5], A. Frey[8], A. Fürtjes[8], D.I. Futyan[16], P. Gagnon[12], J.W. Gary[4], G. Gaycken[25], C. Geich-Gimbel[3], G. Giacomelli[2], P. Giacomelli[8], D. Glenzinski[9], J. Goldberg[21], C. Grandi[2], K. Graham[26], E. Gross[24], J. Grunhaus[22], M. Gruwé[25], P.O. Günther[3], C. Hajdu[29], G.G. Hanson[12], M. Hansroul[8], M. Hapke[13], K. Harder[25], A. Harel[21], M. Harin-Dirac[4], A. Hauke[3], M. Hauschild[8], C.M. Hawkes[1], R. Hawkings[8], R.J. Hemingway[6], C. Hensel[25], G. Herten[10], R.D. Heuer[25], J.C. Hill[5], A. Hocker[9], K. Hoffman[8], R.J. Homer[1], A.K. Honma[8], D. Horváth[29,c], K.R. Hossain[28], R. Howard[27], P. Hüntemeyer[25], P. Igo-Kemenes[11], K. Ishii[23], F.R. Jacob[20], A. Jawahery[17], H. Jeremie[18], C.R. Jones[5], P. Jovanovic[1], T.R. Junk[6], N. Kanaya[23], J. Kanzaki[23], G. Karapetian[18], D. Karlen[6], V. Kartvelishvili[16], K. Kawagoe[23], T. Kawamoto[23], R.K. Keeler[26], R.G. Kellogg[17], B.W. Kennedy[20], D.H. Kim[19], K. Klein[11], A. Klier[24], S. Kluth[32], T. Kobayashi[23], M. Kobel[3], T.P. Kokott[3], S. Komamiya[23], R.V. Kowalewski[26], T. Kress[4], P. Krieger[6], J. von Krogh[11], T. Kuhl[3], M. Kupper[24], P. Kyberd[13], G.D. Lafferty[16], H. Landsman[21], D. Lanske[14], I. Lawson[26], J.G. Layter[4], A. Leins[31], D. Lellouch[24], J. Letts[12], L. Levinson[24], R. Liebisch[11], J. Lillich[10], B. List[8], C. Littlewood[5], A.W. Lloyd[1], S.L. Lloyd[13], F.K. Loebinger[16], G.D. Long[26], M.J. Losty[7], J. Lu[27], J. Ludwig[10], A. Macchiolo[18], A. Macpherson[28,m], W. Mader[3], S. Marcellini[2], T.E. Marchant[16], A.J. Martin[13], J.P. Martin[18], G. Martinez[17], T. Mashimo[23], P. Mättig[24], W.J. McDonald[28], J. McKenna[27], T.J. McMahon[1], R.A. McPherson[26], F. Meijers[8], P. Mendez-Lorenzo[31], W. Menges[25], F.S. Merritt[9], H. Mes[7], A. Michelini[2], S. Mihara[23], G. Mikenberg[24], D.J. Miller[15], W. Mohr[10], A. Montanari[2], T. Mori[23], K. Nagai[8], I. Nakamura[23], H.A. Neal[12,f], R. Nisius[8], S.W. O'Neale[1], F.G. Oakham[7], F. Odorici[2], H.O. Ogren[12], A. Oh[8], A. Okpara[11], M.J. Oreglia[9], S. Orito[23], G. Pásztor[8,j], J.R. Pater[16], G.N. Patrick[20], J. Patt[10], P. Pfeifenschneider[14,i], J.E. Pilcher[9], J. Pinfold[28], D.E. Plane[8], B. Poli[2], J. Polok[8], O. Pooth[8], M. Przybycień[8,d], A. Quadt[8], C. Rembser[8], P. Renkel[24], H. Rick[4], N. Rodning[28], J.M. Roney[26], S. Rosati[3], K. Roscoe[16], A.M. Rossi[2], Y. Rozen[21], K. Runge[10], O. Runolfsson[8], D.R. Rust[12], K. Sachs[6], T. Saeki[23], O. Sahr[31], E.K.G. Sarkisyan[22], C. Sbarra[26], A.D. Schaile[31], O. Schaile[31], P. Scharff-Hansen[8], M. Schröder[8], M. Schumacher[25], C. Schwick[8], W.G. Scott[20], R. Seuster[14,h], T.G. Shears[8,k], B.C. Shen[4], C.H. Shepherd-Themistocleous[5], P. Sherwood[15], G.P. Siroli[2], A. Skuja[17], A.M. Smith[8], G.A. Snow[17], R. Sobie[26], S. Söldner-Rembold[10,e], S. Spagnolo[20], M. Sproston[20], A. Stahl[3], K. Stephens[16], K. Stoll[10], D. Strom[19], R. Ströhmer[31], L. Stumpf[26], B. Surrow[8], S.D. Talbot[1], S. Tarem[21], R.J. Taylor[15], R. Teuscher[9], M. Thiergen[10], J. Thomas[15], M.A. Thomson[8], E. Torrence[9], S. Towers[6], D. Toya[23], T. Trefzger[31], I. Trigger[8], Z. Trócsányi[30,g], E. Tsur[22], M.F. Turner-Watson[1], I. Ueda[23], B. Vachon26, P. Vannerem[10], M. Verzocchi[8], H. Voss[8], J. Vossebeld[8], D. Waller[6], C.P. Ward[5], D.R. Ward[5], P.M. Watkins[1], A.T. Watson[1], N.K. Watson[1], P.S. Wells[8], T. Wengler[8], N. Wermes[3], D. Wetterling[11] J.S. White[6], G.W. Wilson[16], J.A. Wilson[1], T.R. Wyatt[16], S. Yamashita[23], V. Zacek[18], D. Zer-Zion[8,l]

[1]School of Physics and Astronomy, University of Birmingham, Birmingham B15 2TT, UK
[2]Dipartimento di Fisica dell' Università di Bologna and INFN, I-40126 Bologna, Italy
[3]Physikalisches Institut, Universität Bonn, D-53115 Bonn, Germany
[4]Department of Physics, University of California, Riverside CA 92521, USA
[5]Cavendish Laboratory, Cambridge CB3 0HE, UK
[6]Ottawa-Carleton Institute for Physics, Department of Physics, Carleton University, Ottawa, Ontario K1S 5B6, Canada
[7]Centre for Research in Particle Physics, Carleton University, Ottawa, Ontario K1S 5B6, Canada
[8]CERN, European Organisation for Nuclear Research, CH-1211 Geneva 23, Switzerland
[9]Enrico Fermi Institute and Department of Physics, University of Chicago, Chicago IL 60637, USA
[10]Fakultät für Physik, Albert Ludwigs Universität, D-79104 Freiburg, Germany
[11]Physikalisches Institut, Universität Heidelberg, D-69120 Heidelberg, Germany
[12]Indiana University, Department of Physics, Swain Hall West 117, Bloomington IN 47405, USA
[13]Queen Mary and Westfield College, University of London, London E1 4NS, UK
[14]Technische Hochschule Aachen, III Physikalisches Institut, Sommerfeldstrasse 26-28, D-52056 Aachen, Germany
[15]University College London, London WC1E 6BT, UK
[16]Department of Physics, Schuster Laboratory, The University, Manchester M13 9PL, UK
[17]Department of Physics, University of Maryland, College Park, MD 20742, USA
[18]Laboratoire de Physique Nucléaire, Université de Montréal, Montréal, Quebec H3C 3J7, Canada
[19]University of Oregon, Department of Physics, Eugene OR 97403, USA
[20]CLRC Rutherford Appleton Laboratory, Chilton, Didcot, Oxfordshire OX11 0QX, UK
[21]Department of Physics, Technion-Israel Institute of Technology, Haifa 32000, Israel
[22]Department of Physics and Astronomy, Tel Aviv University, Tel Aviv 69978, Israel
[23]International Centre for Elementary Particle Physics and Department of Physics, University of Tokyo, Tokyo 113-0033, and Kobe University, Kobe 657-8501, Japan
[24]Particle Physics Department, Weizmann Institute of Science, Rehovot 76100, Israel
[25]Universität Hamburg/DESY, II Institut für Experimental Physik, Notkestrasse 85, D-22607 Hamburg, Germany
[26]University of Victoria, Department of Physics, P O Box 3055, Victoria BC V8W 3P6, Canada
[27]University of British Columbia, Department of Physics, Vancouver BC V6T 1Z1, Canada
[28]University of Alberta, Department of Physics, Edmonton AB T6G 2J1, Canada
[29]Research Institute for Particle and Nuclear Physics, H-1525 Budapest, P O Box 49, Hungary
[30]Institute of Nuclear Research, H-4001 Debrecen, P O Box 51, Hungary
[31]Ludwigs-Maximilians-Universität München, Sektion Physik, Am Coulombwall 1, D-85748 Garching, Germany
[32]Max-Planck-Institute für Physik, Föhring Ring 6, 80805 München, Germany

[a] and at TRIUMF, Vancouver, Canada V6T 2A3
[b] and Royal Society University Research Fellow
[c] and Institute of Nuclear Research, Debrecen, Hungary
[d] and University of Mining and Metallurgy, Cracow
[e] and Heisenberg Fellow
[f] now at Yale University, Dept of Physics, New Haven, USA
[g] and Department of Experimental Physics, Lajos Kossuth University, Debrecen, Hungary
[h] and MPI München
[i] now at MPI für Physik, 80805 München
[j] and Research Institute for Particle and Nuclear Physics, Budapest, Hungary
[k] now at University of Liverpool, Dept of Physics, Liverpool L69 3BX, UK
[l] and University of California, Riverside, High Energy Physics Group, CA 92521, USA

[m] and CERN, EP Div, 1211 Geneva 23.

1 Introduction

We report measurements of the properties of W pair production in e^+e^- collisions using data recorded by the OPAL detector at LEP at a centre-of-mass energy of 189 GeV with a total integrated luminosity of 183 pb^{-1}. We perform a spin density matrix (SDM) analysis [1,2] of the production and decay properties of the W bosons using the semi-leptonic $WW \to qqe\nu$, $WW \to qq\mu\nu$ and $WW \to qq\tau\nu$ final states. Using suitable summations of SDM elements we present measurements of the inclusive production cross-sections for each of the transverse and longitudinal polarisation states of the W. The SDM elements are also sensitive to triple gauge couplings. We present measurements of CP-violating couplings involving the $W^\pm$, Z^0 and photon.

The doubly resonant $e^+e^- \to W^+W^-$ production process proceeds via s-channel Z^0 or photon exchange, or via t-channel neutrino exchange, collectively known as the CC03 diagrams. The s-channel processes contain the WWZ and WWγ triple gauge boson vertices. The most general Lorentz invariant Lagrangian describing these vertices [3,4] contains 14 independent couplings. In order to facilitate measurements the number of parameters is often reduced to three by assuming $SU(2)_L \times U(1)_Y$ gauge invariance and charge conjugation (C) and parity (P) invariance. The resulting independent couplings are conventionally taken as: $\Delta\kappa_\gamma$, Δg_1^z and λ [5]. Measurements of these couplings using data recorded at LEP2 [6–10] and the Tevatron [11] have been reported elsewhere.

If C, P and CP-invariance are not assumed then several additional couplings may be present. The CP-violating ones can be taken as $\tilde{\kappa}_V$ and $\tilde{\lambda}_V$ which violate P and conserve C, and g_4^V which violates C but conserves P (V = Z^0 or γ) [3]. A further parameter, g_5^V , violates both C and P but conserves CP so is not considered here. $SU(2)_L \times U(1)_Y$ symmetry imposes the following relations [12–14] which are assumed in this analysis:

$$\begin{aligned} \tilde{\kappa}_z &= -\tan^2\theta_w \tilde{\kappa}_\gamma \\ \tilde{\lambda}_z &= \tilde{\lambda}_\gamma \\ g_4^z &= g_4^\gamma \end{aligned} \qquad (1)$$

All of the triple gauge boson couplings (TGCs) can in principle be measured through observations of the W production angular distribution, and distributions of the W decay products. One way of realising such an analysis is through the spin density matrix (SDM) approach. In this approach the individual contributions to the W production angular distribution arising from each of the different possible helicity states of the W bosons can in principle be determined exclusively. These exclusive SDM distributions exhibit different behaviour with respect to each of the TGCs. The TGCs can therefore be determined from the SDM elements in a second step. In W boson pair production, the SDM analysis is particularly suited to the extraction of the CP-violating couplings. Indeed, the imaginary parts of the off-diagonal elements of the SDM are completely insensitive to the CP-conserving couplings, and will only deviate from their Standard Model predictions in the presence of CP-violation at the triple gauge boson vertex.

Before proceeding to the TGC measurements we investigate the exclusive production cross-sections for each of the transverse and longitudinal polarisations of W bosons. These can be made in the context of the SDM analysis by suitable summations of SDM elements which are described in detail in the following section. The study of the longitudinal cross-section is particularly interesting as this degree of freedom of the W only arises in the Standard Model through the electro-weak symmetry breaking mechanism. Previous measurements of the proportion of longitudinally polarised W bosons produced at LEP2 have been been reported by the OPAL [9] and L3 [15] experiments.

In addition we present limits on the CP-violating parameters. Previous limits on the CP-violating

TGCs have been obtained at the DELPHI experiment using data at 161 GeV and 172 GeV [8]. Limits on the CP-violating WWγ couplings, $\tilde{\kappa}_\gamma$ and $\tilde{\lambda}_\gamma$, have been obtained at the D0 experiment [16] from the process $\mathrm{p\bar{p}} \rightarrow \ell\nu\gamma + \mathrm{X}$. Measurements of the neutron electric dipole moment show that the electromagnetic interaction is CP-conserving to very high accuracy [17].

2 The Spin Density Matrix

The two-particle joint spin density matrix (SDM) [4] describes the contribution of each of the helicity states of the W bosons to the $\mathrm{W^+W^-}$ production cross-section.

The amplitude for the production of a $\mathrm{W^-}$ with helicity τ_- ($= -1$,0 or 1) and a $\mathrm{W^+}$ with helicity τ_+ is denoted as $F^{(\lambda)}_{\tau_-\tau_+}(s,\cos\theta_\mathrm{W})$ [1,4], where λ ($= \pm\frac{1}{2}$) denotes the helicity of the $\mathrm{e^-}$, s is the square of the centre-of-mass energy and $\cos\theta_\mathrm{W}$ is the W production angle in the centre-of-mass frame. The SDM (ρ) elements are normalised products of these amplitudes given by [4]:

$$\rho_{\tau_-\tau'_-\tau_+\tau'_+}(s,\cos\theta_\mathrm{W}) = \frac{\sum_\lambda F^{(\lambda)}_{\tau_-\tau_+}(F^{(\lambda)}_{\tau'_-\tau'_+})^*}{\sum_{\lambda\tau_+\tau_-}|F^{(\lambda)}_{\tau_-\tau_+}|^2} \qquad (2)$$

The normalisation ensures that $\sum_{\tau_-\tau_+}\rho_{\tau_-\tau_-\tau_+\tau_+} = 1$. The ρ matrix is Hermitian, giving 80 independent real coefficients which may be experimentally measured. The diagonal elements are defined as the subset of elements where $\tau_- = \tau'_-$ and $\tau_+ = \tau'_+$. These diagonal elements are purely real and are equivalent to the probability of producing a final $\mathrm{W^+W^-}$ state with helicities τ_+ and τ_- respectively. The off-diagonal elements represent interference terms between the different helicity states of each W.

In the context of a limited sample of events it may not be possible to measure all of the components independently. It is then useful to consider the single particle density matrix for either the $\mathrm{W^-}$ or $\mathrm{W^+}$, formed by summation over the helicity states of the other W. For example the $\mathrm{W^-}$ matrix elements $\rho^{W^-}_{\tau_-\tau'_-}$ are obtained by summation over $\tau_+ = \tau'_+$:

$$\rho^{W^-}_{\tau_-\tau'_-}(s,\cos\theta_\mathrm{W}) = \sum_{\tau_+}\rho_{\tau_-\tau'_-\tau_+\tau_+}(s,\cos\theta_\mathrm{W}) \qquad (3)$$

The Hermitian matrix ρ^{W^-} has eight independent real coefficients, and satisfies the normalisation constraint $\sum_{\tau_-}\rho^{W^-}_{\tau_-\tau_-} = 1$. The three real diagonal elements represent the relative production probabilities for a final state $\mathrm{W^-}$ with a particular helicity.

The constraints of CPT and CP-invariance impose additional symmetries on the density matrix at tree level [2]. CPT-invariance imposes the conditions:

$$\mathrm{Re}(\rho^{W^-}_{\tau_1\tau_2}) \;-\; \mathrm{Re}(\rho^{W^+}_{-\tau_1-\tau_2}) = 0 \qquad (4)$$

$$\mathrm{Im}(\rho^{W^-}_{\tau_1\tau_2}) \;+\; \mathrm{Im}(\rho^{W^+}_{-\tau_1-\tau_2}) = 0 \qquad (5)$$

CP invariance imposes the condition:

$$\mathrm{Im}(\rho^{W^-}_{\tau_1\tau_2}) \;-\; \mathrm{Im}(\rho^{W^+}_{-\tau_1-\tau_2}) = 0 \qquad (6)$$

Thus CPT and CP-conservation together dictate that all coefficients from $\rho^{W}_{\tau_1\tau_2}$ are real. Deviations from the validity of equation (6) would represent an unambiguous signal for CP-violation at tree level.

Deviations from the equality of equation (5) represent a signal of higher-order (loop) effects beyond tree level [2].

The exclusive differential cross-sections for the production of a W with transverse (T) or longitudinal (L) helicity are obtained by weighting the total differential cross-section by the relevant elements of the single particle ρ matrix:

$$\begin{aligned} \frac{\mathrm{d}\sigma_{\mathrm{T}}}{\mathrm{d}\cos\theta_{\mathrm{W}}} &= (\rho_{++}+\rho_{--})\frac{\mathrm{d}\sigma}{\mathrm{d}\cos\theta_{\mathrm{W}}} \\ \frac{\mathrm{d}\sigma_{\mathrm{L}}}{\mathrm{d}\cos\theta_{\mathrm{W}}} &= (\rho_{00})\frac{\mathrm{d}\sigma}{\mathrm{d}\cos\theta_{\mathrm{W}}} \end{aligned} \tag{7}$$

and the corresponding total cross-sections are given by:

$$\begin{aligned} \sigma_{\mathrm{T}} &= \int_{-1}^{+1}(\rho_{++}+\rho_{--})\frac{\mathrm{d}\sigma}{\mathrm{d}\cos\theta_{\mathrm{W}}}\mathrm{d}\cos\theta_{\mathrm{W}} \\ \sigma_{\mathrm{L}} &= \int_{-1}^{+1}(\rho_{00})\frac{\mathrm{d}\sigma}{\mathrm{d}\cos\theta_{\mathrm{W}}}\mathrm{d}\cos\theta_{\mathrm{W}}\,. \end{aligned} \tag{8}$$

The single W SDM elements can be obtained from measurements of the properties of the W decay products by the application of suitable projection operators $\Lambda_{\tau\tau'}$ [1,2] which assume the V$-$A coupling of the W to fermions. The W decays are characterised by the polar and azimuthal angles of the decay fermion in the W rest frame, θ^* and ϕ^* respectively. In this analysis we consider only the semi-leptonic event class, $\mathrm{WW}\to \mathrm{q}\mathrm{q}\ell\nu$, where one W decays to a lepton (e, μ or τ) and a neutrino and the other to two hadronic jets. In this case the values of θ^* and ϕ^* of the lepton may be determined unambiguously and the corresponding single W SDM elements are given by:

$$\begin{aligned} &\frac{\mathrm{d}\sigma(\mathrm{e}^+\mathrm{e}^-\to\mathrm{W}^+\mathrm{W}^-)}{\mathrm{d}\cos\theta_{\mathrm{W}}}\rho^{W^-}_{\tau\tau'} \\ &= \frac{1}{\mathrm{Br}(\mathrm{W}^-\to\ell^-\bar{\nu})}\int\frac{\mathrm{d}\sigma(\mathrm{e}^+\mathrm{e}^-\to W^+\ell^-\bar{\nu})}{\mathrm{d}\cos\theta_{\mathrm{W}}\mathrm{d}\cos\theta^*\mathrm{d}\phi^*}\Lambda_{\tau\tau'}(\theta^*,\phi^*)\mathrm{d}\cos\theta^*\mathrm{d}\phi^* \end{aligned} \tag{9}$$

In section 4 we describe how this expression is realised as a sum over the events observed in the data sample.

In the case of the hadronically decaying W differentiation between the particle and anti-particle decay products is very difficult. However, certain projection operators are symmetric under the transformation $\cos\theta^*\to-\cos\theta^*$, $\phi^*\to\phi^*+\pi$, i.e. the interchange of one of the decay particles from the W boson with the other decay particle, for example the u-type quark with the d-type in a hadronically decaying W boson. This means that a number of combinations of the SDM elements may still be extracted from $\mathrm{W}\to \mathrm{q}\bar{\mathrm{q}}$ decays: these include $\rho_{++}+\rho_{--}$ and ρ_{00}. Both W bosons in the event can therefore be used to measure the polarised cross-section, since only these terms appear in equations (7).

Returning to the full two particle SDM, the analogous expressions to (7) but describing the differential cross-section for both W bosons in the pair being transversely polarised (TT), both being longitudinally polarised (LL), or one of each polarisation (TL) are:

$$\begin{aligned} \frac{\mathrm{d}\sigma_{\mathrm{TT}}}{\mathrm{d}\cos\theta_{\mathrm{W}}} &= (\rho_{++++}+\rho_{++--}+\rho_{--++}+\rho_{----})\frac{\mathrm{d}\sigma}{\mathrm{d}\cos\theta_{\mathrm{W}}} \\ \frac{\mathrm{d}\sigma_{\mathrm{LL}}}{\mathrm{d}\cos\theta_{\mathrm{W}}} &= (\rho_{0000})\frac{\mathrm{d}\sigma}{\mathrm{d}\cos\theta_{\mathrm{W}}} \\ \frac{\mathrm{d}\sigma_{\mathrm{TL}}}{\mathrm{d}\cos\theta_{\mathrm{W}}} &= (\rho_{++00}+\rho_{--00}+\rho_{00++}+\rho_{00--})\frac{\mathrm{d}\sigma}{\mathrm{d}\cos\theta_{\mathrm{W}}} \end{aligned} \tag{10}$$

and the analogous expression to (9) is

$$\begin{aligned}
&\frac{\mathrm{d}\sigma(\mathrm{e^+e^-}\to\mathrm{W^+W^-})}{\mathrm{d}\cos\theta_{\mathrm{W}}}\rho_{\tau_-\tau'_-\tau_+\tau'_+}\\
=\;&\frac{1}{\mathrm{Br}(\mathrm{W}\to\mathrm{qq})\mathrm{Br}(\mathrm{W}\to\ell\nu)}\int\frac{\mathrm{d}\sigma(\mathrm{e^+e^-}\to\mathrm{qq}\ell\nu)}{\mathrm{d}\cos\theta_{\mathrm{W}}\mathrm{d}\cos\theta^*_-\mathrm{d}\phi^*_-\mathrm{d}\cos\theta^*_+\mathrm{d}\phi^*_+}\\
\times\;&\Lambda_{\tau_-\tau'_-}(\theta^*_-,\phi^*_-)\Lambda_{\tau_+\tau'_+}(\theta^*_+,\phi^*_+)\mathrm{d}\cos\theta^*_-\mathrm{d}\phi^*_-\mathrm{d}\cos\theta^*_+\mathrm{d}\phi^*_+
\end{aligned}\qquad(11)$$

where the integral is now over the decay angles of both W bosons.

3 The Data Sample and Monte Carlo Simulated Events

3.1 The Data Sample

The W-pair data used in this analysis were collected by the OPAL [18] detector at LEP. The accepted integrated luminosity in 1998, evaluated using small angle Bhabha scattering events observed in the silicon tungsten forward calorimeter [19], is 183.14 $\pm$ 0.55 pb^{-1} [20]. The luminosity-weighted mean centre-of-mass energy for the data sample is $\sqrt{s} = 188.64 \pm 0.04$ GeV.

In this analysis we use only the W-pair events decaying to the qqeν, qq$\mu\nu$ and qq$\tau\nu$ channels. These qq$\ell\nu$ events were first selected using the likelihood selection described in [9, 20, 21]. The selection is designed to optimise the rejection of $\mathrm{Z}^0/\gamma \to \mathrm{q\bar{q}}$ and four-fermion backgrounds. A total of 1252 qq$\ell\nu$ candidates was selected at this stage. Monte Carlo studies show this selection is about 88% efficient.

Further cuts are applied in order to obtain a sample of well reconstructed events. A full description can be found in [10]. A brief overview of the procedure is given here. For the qqeν and qq$\mu\nu$ events a well reconstructed lepton track is required. For the qq$\tau\nu$ events, either one track or a narrow jet consisting of three tracks is assigned as the τ decay product.

Kinematic fits are now applied to the events. For the qqeν and qq$\mu\nu$ events a one-constraint fit is applied that requires energy-momentum conservation and neglects any initial state radiation. Events are accepted if the fit converges with a probability larger than 0.001. An improvement is made to the resolution of the angular observables by performing a second kinematic fit which constrains each reconstructed W mass to the average value measured at the Tevatron [22]. Events for which the fit converges with a probability of at least 0.001 are accepted; for other events we revert to the previous fit.

For the qq$\tau\nu$ events a different kinematic fit is applied [9]; here the reconstructed mass of the two W bosons is required to be equal. In order to obtain a W mass from the leptonic part of these events, it is necessary to assume that the direction of the visible part of the τ decay approximates the direction of the τ lepton. The fit is required to converge with a probability of at least 0.025. This cut rejects 41% of the background. It also rejects about 14% of the signal events, but preferentially rejects events where the τ decay products are not correctly identified.

After application of all selection cuts 1065 qq$\ell\nu$ candidates remain, with 359 in the qqeν channel, 386 in the qq$\mu\nu$ channel and 320 in the qq$\tau\nu$ channel. The W production and decay angles for these events are shown in figure 1. The background contributions to the data sample are estimated using Monte Carlo samples. The resulting contaminations are expected to be four-fermion (non-CC03) 3.1%,

$Z^0/\gamma \to q\bar{q}$ 2.1%, two-photon (multiperipheral) 0.2% and CC03 four-fermion (WW $\to$ qqqq and $\ell\nu\ell\nu$) 0.5%.

3.2 Monte Carlo

A number of Monte Carlo models are used to provide estimates of efficiencies and backgrounds as well as the expected W-pair production and decay angular distributions for different TGC values. The Monte Carlo samples are generated at $\sqrt{s}$ = 189 GeV. All Monte Carlo samples mentioned below are passed through the full OPAL simulation program [23] and then subjected to the same selection and reconstruction procedure as the data. The ERATO [13] Monte Carlo program is used in this analysis because it can generate samples of four-fermion Monte Carlo events with non-Standard Model values of CP-violating anomalous couplings. The EXCALIBUR [24] Monte Carlo is also used extensively in this analysis for correction of detector effects and as the main tool to compare to the 189 GeV data. A comparison between ERATO and EXCALIBUR angular distributions and spin density matrix elements was undertaken and no statistically significant differences were seen between them. The other four-fermion generator used to calculate background contributions and systematic uncertainties is grc4f [25]. The WW generators used to calculate theoretical predictions for the W-pair polarisations and to calculate systematic uncertainties are EXCALIBUR, HERWIG [26], PYTHIA [27] and KORALW [28]. The background $Z^0/\gamma \to q\bar{q}$ samples are generated using PYTHIA. For samples of two-photon (multiperipheral) background PYTHIA, PHOJET [29] and HERWIG were used.

4 Measurement of W Boson Polarisation

4.1 Experimental Method

Measurements of the production cross-sections for each of the transverse and longitudinal states of the W bosons are obtained from summations of the SDM elements obtained from the qq$\ell\nu$ data sample, after correcting for detector acceptance, resolution effects and background contamination.

To calculate the SDM elements the events are divided into eight equal bins, k, of $\cos\theta_{\mathrm{W}}$. In each bin the SDM elements are obtained by a summation over events, i, weighted by the relevant SDM projection operators as shown in equation (12). This is effectively the realisation of equation (9) as a summation over observed events. N_k is the number of events in bin k. In the extraction of all the individual W SDM elements CPT invariance is assumed, so all leptonic (hadronic) W^+ and W^- decays can be combined.

$$\rho^k_{\tau\tau'}(\cos\theta^k_W) = \frac{1}{N_k}\sum_{i=1}^{N_k} \Lambda_{\tau\tau'}(\cos\theta^*_i, \phi^*_i) \tag{12}$$

Estimates of the production cross-sections are derived from the diagonal SDM elements; therefore the projection operators only involve the polar decay angle $\cos\theta^*$. It is not required that the SDM elements be positive definite. Both the leptonic and hadronic W decays can be used since the SDM combinations occurring in equation (7) are symmetric with respect to the use of the fermion or anti-fermion polar decay angle. Each event is also weighted by a correction factor, f, for detector acceptance and resolution effects:

$$\rho^k_{00} = \frac{1}{N^{\mathrm{cor}}_k}\sum_{i=1}^{N_k} \frac{1}{f_k(\theta^*_i)}\Lambda_{00}(\theta^*_i) \tag{13}$$

$$\rho^k_{++} + \rho^k_{--} = \frac{1}{N^{\mathrm{cor}}_k} \sum_{i=1}^{N_k} \frac{1}{f_k(\theta^*_i)} (\Lambda_{++}(\theta^*_i) + \Lambda_{--}(\theta^*_i)) \tag{14}$$

where N^{cor}_k is the corrected number of events in bin k:

$$N^{\mathrm{cor}}_k = \sum_{i=1}^{N_k} \frac{1}{f_k(\theta^*_i)}. \tag{15}$$

The factors $f_k(\theta^*_i)$ are obtained from fully simulated Monte Carlo events, and are calculated as a function of $\cos\theta_{\mathrm{W}}$ and $\cos\theta^*$. They are defined to be the ratio of the number of reconstructed events to the number of generated events in each bin. The correction factors have an effect of between 5% and 20%. The typical resolution of the measured $\cos\theta_{\mathrm{W}}$ is found to be 0.05, which is less than 20% of the bin width used in correcting this distribution. The typical resolution of the measured $\cos\theta^*$ is found to be 0.07, which is 70% of the bin width used in the calculation of the correction factors.

The distribution of uncorrected events, shown in figure 1, also has to be corrected for detector acceptance and resolution effects. This is done in a similar manner to the correction of the SDM elements by calculating a correction factor from Monte Carlo events in a bin-wise fashion and applying it to the data. The estimated background contribution is subtracted from the SDM elements and the $\mathrm{d}\sigma/\mathrm{d}\cos\theta_{\mathrm{W}}$ distribution.

The polarised differential cross-sections, $\mathrm{d}\sigma_{\mathrm{L}}/\mathrm{d}\cos\theta_{\mathrm{W}}$ and $\mathrm{d}\sigma_{\mathrm{T}}/\mathrm{d}\cos\theta_{\mathrm{W}}$, are then obtained by multiplying the binned unpolarised differential cross-section by the relevant SDM combinations, following equations (7).

4.2 Experimental Results

Figure 2 shows the individual W boson differential cross-sections obtained from the data by this method. The transverse and longitudinal components obtained from the leptonically decaying W and the hadronically decaying W are shown separately, together with the values obtained by combining the two. The polarisations of the W bosons in the W-pair event are correlated. The correlation is estimated to be 0.07, and is taken into account in the errors on the combined cross-sections.

The fraction of each polarisation state, obtained by integrating over $\cos\theta_{\mathrm{W}}$ and then dividing by the total cross-section, is given in table 1. Once again the correlated polarisations of the two W bosons are taken into account when deriving the errors. The estimation of the systematic errors shown in tables 1 and 2 is described in section 6.

The joint polarised cross-sections are obtained by extracting the joint SDM elements in a similar way to equations (12)

$$\rho^k_{\tau_-\tau'_-\tau_+\tau'_+} = \frac{1}{N^{cor}_k} \sum_{i=1}^{N_k} \frac{1}{f_k(\theta^{*\mathrm{lept}}_i, \theta^{*\mathrm{had}}_i)} \Lambda^{\mathrm{W}^\pm}_{\tau_-\tau'_-}(\theta^{*\mathrm{lept}}_i) \Lambda^{\mathrm{W}^\mp}_{\tau_+\tau'_+}(\theta^{*\mathrm{had}}_i) \tag{16}$$

where in this case the ρ and Λ are those corresponding to the particular SDM combinations appearing in equation (10). Note that there is now a projection operator for each W, and the correction factor is binned in terms of both polar decay angles. Figure 3 shows the joint differential cross-sections obtained by this method, these cross-sections are not constrained to be positive definite.

The fractions of each helicity state, obtained by integrating over $\cos\theta_{\mathrm{W}}$ of the W and then dividing by the total cross-section, are shown in table 2. These results are highly correlated. The correlations

	$\sigma_{\mathrm{T}}/\sigma_{\mathrm{total}}$	$\sigma_{\mathrm{L}}/\sigma_{\mathrm{total}}$
Data		
W→ $\ell\nu$	$0.842 \pm 0.048 \pm 0.023$	$0.158 \pm 0.048 \pm 0.023$
W→ qq	$0.738 \pm 0.045 \pm 0.025$	$0.262 \pm 0.045 \pm 0.025$
All	$0.790 \pm 0.033 \pm 0.016$	$0.210 \pm 0.033 \pm 0.016$
Standard Model Expectation		
W→ $\ell\nu$	0.746 ± 0.006	0.254 ± 0.006
W→ qq	0.741 ± 0.006	0.259 ± 0.006
All	0.743 ± 0.004	0.257 ± 0.004

Table 1: The fractions of transversely and longitudinally polarised W bosons. The expected values are from generator level EXCALIBUR Monte Carlo, the errors being statistical only. The first error on the measured values is statistical and the second is the systematic uncertainty.

between each helicity fraction, calculated from the data, are found to be: $\sigma_{\mathrm{TT}}{:}\sigma_{\mathrm{LL}} = 0.67{\pm}0.02$, $\sigma_{\mathrm{TT}}{:}\sigma_{\mathrm{TL}} = -0.93{\pm}0.01$ and $\sigma_{\mathrm{LL}}{:}\sigma_{\mathrm{TL}} = -0.89{\pm}0.01$.

The individual W polarised differential cross-sections show good agreement with the Standard Model predictions, as do the overall fraction of each individual W polarisation, as seen in table 1. The W pair polarised cross-sections show less good agreement, but $\sigma_{\mathrm{LL}}/\sigma_{\mathrm{total}}$ is within two standard deviations of the Standard Model prediction and the other two are just over two standard deviations away. The χ^2 value for the three measurements compared to the Standard Model expectations, including systematic uncertainties, is 4.7. This corresponds to a χ^2 probability of 10%.

	Measured	Expected
$\sigma_{\mathrm{TT}}/\sigma_{\mathrm{total}}$	$0.781 \pm 0.090 \pm 0.033$	0.572 ± 0.010
$\sigma_{\mathrm{LL}}/\sigma_{\mathrm{total}}$	$0.201 \pm 0.072 \pm 0.018$	0.086 ± 0.008
$\sigma_{\mathrm{TL}}/\sigma_{\mathrm{total}}$	$0.018 \pm 0.147 \pm 0.038$	0.342 ± 0.016

Table 2: The fraction of each helicity combination of WW pairs. The expected values are calculated from Monte Carlo studies. The first errors on the measured fractions are statistical and the second are systematic. The errors on the expected fractions are statistical only.

5 Measurement of Anomalous Couplings and Test of CP-Invariance

Measurements of anomalous coupling parameters are obtained through a comparison of distributions of SDM elements obtained from the leptonically decaying W bosons in the qq$\ell\nu$ data sample with distributions obtained from fully simulated Monte Carlo samples. In contrast to the polarised cross-section measurements, neither data nor Monte Carlo events are corrected for detector or acceptance effects. Instead the experimentally observed SDM distributions are compared directly with those for fully detector simulated Monte Carlo events. Monte Carlo samples for arbitrary TGC values are obtained by a re-weighting technique applied to a large Standard Model sample. A χ^2 minimisation procedure is then used to find the simulated data set which best fits the data and hence obtain the best fit TGC parameter value.

The events are again divided into eight equal bins of $\cos\theta_{\mathrm{W}}$. Equation (12) is used to calculate all six real and three imaginary SDM elements directly. The SDM distributions are shown in figure 4.

This method is used to calculate both the CP-conserving and the CP-violating couplings. However, when performing the fit for CP-conserving couplings only the six real SDM coefficients are used, and in the case of CP violating couplings all nine SDM coefficients are included. The effect of correlations between SDM elements is included. Although there is no correlation between $\cos\theta_{\mathrm{W}}$ bins, within each bin the measurements of the SDM elements are highly correlated. The correlations are obtained directly from the data.

The Monte Carlo sample used in the fitting procedure is generated for Standard Model couplings using EXCALIBUR. All TGC-dependent four-fermion diagrams are included in this sample. SDM distributions for arbitrary couplings are obtained by re-weighting the fully simulated EXCALIBUR Monte Carlo events. Technically this was achieved by re-weighting events with the matrix elements from [1]. The five characteristic W production and decay angles are constructed from the original four-momenta of the primary fermions in the simulated EXCALIBUR events. This treatment neglects the effects of four-fermion background, but these are checked explicitly for CP-conserving couplings, and found to be negligible. The expected contribution from four-fermion background events produced in channels unaffected by triple gauge couplings, and those from other backgrounds, are added to the EXCALIBUR sample.

As the SDM elements are normalised to the number of events in each $\cos\theta_{\mathrm{W}}$ bin, information from the production angle of the W is effectively removed from the SDM fit. In order to include this an independent χ^2 is derived from the comparison of the shape of the $\cos\theta_{\mathrm{W}}$ distributions and this is incorporated into the fit. No information from the overall cross-section is included.

The method of re-weighting and fitting is tested by performing fits to large samples of fully simulated four-fermion Monte Carlo samples generated with various anomalous couplings as well as others generated with Standard Model couplings. These bias tests show that the extracted coupling values are consistent in all cases with the generated values. The reliability of the statistical error is also tested by performing a fit to a large number of subsamples of the Monte Carlo, each with the same statistics as the data. It is found that in the case of the Standard Model Monte Carlo at least 68% of the fitted values of the couplings fall within $\Delta\chi^2$=1 of the Standard Model values of the couplings. Similar tests are performed on samples of Monte Carlo with anomalous couplings. Statistics are lower, but in all cases the results are consistent with the expectation, as seen for the Standard Model samples.

For the CP-violating couplings, including statistical uncertainties and the systematic uncertainties described in section 6, we find:

$$\begin{aligned}\tilde{\kappa}_{\mathrm{z}} &= -0.20^{+0.10}_{-0.07}\\ g_4^{\mathrm{z}} &= -0.02^{+0.32}_{-0.33}\\ \tilde{\lambda}_{\mathrm{z}} &= -0.18^{+0.24}_{-0.16}\end{aligned}$$

and for the CP-conserving couplings we find:

$$\begin{aligned}\Delta\kappa_\gamma &= -0.22^{+0.29}_{-0.24}\\ \Delta g_1^{\mathrm{z}} &= -0.03^{+0.09}_{-0.09}\\ \lambda &= -0.08^{+0.10}_{-0.09}\end{aligned}$$

These latter results are consistent with those measured in [10]. All couplings are set to their Standard Model values except the coupling being measured and those related to it via the $SU(2)_{\mathrm{L}} \times U(1)_{\mathrm{Y}}$ symmetry. A full breakdown of the results for the CP-violating couplings is shown in table 3.

The χ^2 plots for all the fits including systematics can be seen in figure 5. The double minima in the χ^2 curves for the CP-violating couplings derived from the $\cos\theta_{\mathrm{W}}$ distribution alone reflect that the $\cos\theta_{\mathrm{W}}$ distribution is sensitive only to the absolute magnitude of the coupling. The same is true for the real SDM elements resulting in the double minima in the SDM χ^2 curve for $\tilde{\kappa}_Z$. It is only the imaginary parts that lift the degeneracy. It is evident that the CP-violating couplings are better constrained by the SDM elements than by the W boson production angular distribution, whereas for the CP-conserving couplings the converse is true.

A further test of tree level CP violation is given by comparing the imaginary SDM elements from the W^+ to those from the W^-, as in equation (6). These comparisons, which give a model independent test of CP-violation in the triple gauge coupling, are shown in figure 6. Deviations from zero would only be due to CP-violation at tree level. No deviations are seen, complementing the results of the measurements of the CP-violating TGCs.

Also shown in figure 6 are the combinations of imaginary SDM elements that test for effects beyond tree level, as described by equation (5). Any deviation from zero in these plots could only be caused by either loop effects or CPT-violation; all CP-violating tree level effects cancel out. The data are consistent with no effect.

6 Systematic Uncertainties

Systematic uncertainties in the measurements are calculated as described below. The individual contributions to the errors on the polarised cross-section fractions are given in table 4. For the measurements of the TGCs, all error sources listed below are included except that from the detector correction. For all TGC measurements the systematic errors are included as extra uncertainties on the contents of each bin of the SDM element and $\cos\theta_{\mathrm{W}}$ distributions. Each systematic uncertainty is taken to be uncorrelated between bins in both $\cos\theta_{\mathrm{W}}$ and the different SDM element distributions.

• Jet reconstruction: Uncertainties in the modelling of jet reconstruction are estimated by varying the reconstruction in a Monte Carlo sample. The resolutions of the three jet parameters (energy, $\cos\theta_j$, ϕ_j) are varied by 10%, and the energy is shifted by 5% to account for systematic uncertainties. This is done for both the quark jets and the τ jets. The size of the variations for the quark jets is determined from extensive studies of back-to-back jets at Z^0 energies. A possible systematic shift in the reconstructed direction of the boson has been estimated using radiative $\mathrm{Z}^0/\gamma \rightarrow \mathrm{q}\bar{\mathrm{q}}$ events. The possible shift in $|\cos\theta_{\mathrm{W}}|$ was found to be less than 0.01 [10]. The same uncertainties are taken on the τ jets as for the quark jets.

• Hadronisation: Uncertainties due to the hadronisation model are estimated by comparing Monte Carlo fragmented with HERWIG5.9 to Monte Carlo using the JETSET7.4 [27] hadronisation scheme. Both Monte Carlos have been tuned to OPAL data. Variations in the calculated polarised cross-sections, SDM elements and $\cos\theta_{\mathrm{W}}$ distribution between the different samples are taken as the systematic uncertainty.

• Monte Carlo generators: The modelling of the four-fermion production processes is assessed by comparing SDM elements and $\cos\theta_{\mathrm{W}}$ distributions from the ERATO and grc4f Monte Carlo programs to those from EXCALIBUR. All these generators have a different calculation of the matrix elements and a different treatment of ISR. The calculated values of the individual W and W-pair polarised cross-section fractions are also compared. Variations in the calculated polarised cross-sections, SDM elements and $\cos\theta_{\mathrm{W}}$ distribution between the different samples are taken as the systematic uncertainty.

• Background simulation: Possible systematic effects due to the simulation of the dominant Z^0/γ background are accounted for by replacing the PYTHIA Monte Carlo with a HERWIG sample. The two-photon background is removed and doubled as well. Variations in the extracted polarised cross-sections, SDM elements and $\cos\theta_{\mathrm{W}}$ distribution are taken as the systematic uncertainty.

• Lepton ID: The efficiency of the lepton identification in the data compared to that in the Monte Carlo is investigated as a function of the polar angle and energy of the lepton. The Monte Carlo is weighted to adjust these distributions to the data. Variations in the calculated polarised cross-sections, SDM elements and $\cos\theta_{\mathrm{W}}$ distribution between the samples before and after weighting are taken as the systematic uncertainty.

• Detector effect correction: The use of Standard Model Monte Carlo to correct for detector effects could introduce some bias. This is tested for by comparing the helicity fractions calculated from generator level non-Standard Model Monte Carlo with those calculated from the same sample after full detector simulation and correction using correction factors determined from Standard Model Monte Carlo. This test is done with six samples of Monte Carlo each with one of the couplings $\Delta\kappa_{\gamma}$, Δg_1^z, λ, set to ± 1.

• Lepton energy scale and charge misassignment: Uncertainties on the lepton energy scale are tested by shifting the lepton energy by 0.3%. These are found to be negligible. The momentum resolution of electrons and muons and their charge misassignment are investigated by varying the resolution in $\mathrm{Q/p_t}$ by 10%. Here Q is the lepton charge and $\mathrm{p_t}$ is the transverse momentum with respect to the beam direction.

7 Conclusion

W-pair events with one leptonically and one hadronically decaying W are analysed to extract the polarisation properties of the W boson and test CP invariance. Both the individual W, and W-pair, polarised cross-sections have been measured. The individual W polarised cross-sections are well-described by the Standard Model predictions, both inclusively and separately for the leptonically and hadronically decaying W bosons (table 1). The results are consistent with those measured by L3 at the same centre-of-mass energy [15], with the results presented here being more precise.

The W-pair polarised cross-sections are measured for the first time at LEP. All the results are found to be consistent with the Standard Model expectations (table 2).

Triple gauge couplings are extracted using information from the leptonically decaying W, together with the W production polar angle. They are found to be consistent with the Standard Model predictions. The CP conserving couplings have been measured elsewhere with the same data sample [10], and serve as a consistency check for this analysis. The CP violating couplings $\tilde{\kappa}_{\mathrm{z}}$, $\tilde{\lambda}_{\mathrm{z}}$ and g_4^{z} are measured for the first time with OPAL data, table 3, and constraints are thus placed on possible new CP-violating contributions to the W production and decay processes.

Acknowledgements

We particularly wish to thank the SL Division for the efficient operation of the LEP accelerator at all energies and for their continuing close cooperation with our experimental group. We thank our colleagues from CEA, DAPNIA/SPP, CE-Saclay for their efforts over the years on the time-of-flight and trigger systems which we continue to use. In addition to the support staff at our own institutions

we are pleased to acknowledge the
Department of Energy, USA,
National Science Foundation, USA,
Particle Physics and Astronomy Research Council, UK,
Natural Sciences and Engineering Research Council, Canada,
Israel Science Foundation, administered by the Israel Academy of Science and Humanities,
Minerva Gesellschaft,
Benoziyo Center for High Energy Physics,
Japanese Ministry of Education, Science and Culture (the Monbusho) and a grant under the Monbusho International Science Research Program,
Japanese Society for the Promotion of Science (JSPS),
German Israeli Bi-national Science Foundation (GIF),
Bundesministerium für Bildung und Forschung, Germany,
National Research Council of Canada,
Research Corporation, USA,
Hungarian Foundation for Scientific Research, OTKA T-029328, T023793 and OTKA F-023259.

References

[1] G. Gounaris, J. Layssac, G. Moultaka and F.M. Renard, Int. J. Mod. Phys. **A8**, (1993) 3285.

[2] G. Gounaris, D. Schildknecht and F. M. Renard, Phys. Lett. **B263**, (1991) 291.

[3] K. Hagiwara *et al.*, Nucl. Phys. **B282** (1987) 253.

[4] M. Bilenkii, J. L. Kneur, F. M. Renard and D. Schildknecht, Nucl. Phys. **B409** (1993) 22.

[5] Physics at LEP2, edited by G. Altarelli, T. Sjostrand and F. Zwirner, CERN 96-01 Vol. 1, 525.

[6] DELPHI Collaboration, P. Abreu *et al.,* Phys. Lett. **B397** (1997) 158;
L3 Collaboration, M. Acciarri *et al.,* Phys. Lett. **B398** (1997) 223;
L3 Collaboration, M. Acciarri *et al.,* Phys. Lett. **B413** (1997) 176;
OPAL Collaboration, G. Abbiendi *et al.,* Phys. Lett. **B397** (1997) 147;
ALEPH Collaboration, R. Barate *et al.,* Phys. Lett. **B422** (1998) 369;
DELPHI Collaboration, P. Abreu *et al.,* Phys. Lett. **B459** (1999) 382;
L3 Collaboration, M. Acciarri *et al.,* CERN-EP/99-131, *submitted to Phys. Lett. B.*

[7] OPAL Collaboration, K. Ackerstaff *et al.,* Eur. Phys J. **C2**, (1998) 597.

[8] DELPHI Collaboration, P. Abreu *et al.,* Phys.Lett. **B423**, (1998) 194.

[9] OPAL Collaboration, G. Abbiendi *et al.,* Eur. Phys. J. **C8** (1999) 191.

[10] OPAL Collaboration,G. Abbiendi *et al.,* "Measurement of Triple Gauge Boson Couplings from W^+W^- Production at LEP Energies up to 189 GeV," CERN-EP-2000-114, *Submitted to Eur. Phys. J. C.*.

[11] CDF Collaboration, F. Abe *et al.,* Phys. Rev. Lett. **78** (1997) 4536;
D0 Collaboration, B Abbott *et al.,* Phys. Rev. **D58** (1998) 31102.

[12] G. Gounaris, C. G. Papadopoulos, Eur. Phys. J. **C2** (1998) 365.

[13] C. G. Papadopoulos, Comput. Phys. Commun. **101**, (1997) 183.

[14] G. Gounaris, private communication.

[15] L3 Collaboration, M. Acciarri *et al.* Phys. Lett. **B474** (2000) 194.

[16] D0 Collaboration, S. Abachi *et al.,* Phys. Rev. Lett. **78** (1997) 3634.

[17] P. G. Harris *et al.,* Phys Rev. Lett. **82**, (1999) 904;
K. F. Smith *et al.,* Phys. Lett. **B234**, (1990) 191.

[18] OPAL Collaboration, K. Ahmet *et al.* Nucl. Instrum. Meth. **A305** (1991) 275.

[19] B. E. Anderson *et al.*, IEEE Trans. Nucl. Sci. **41** (1994) 845.

[20] OPAL Collaboration, G Abbiendi *et al.,* "W^+W^- Production Cross Section and W Branching Fractions in e^+e^- Collisions at 189 GeV," CERN-EP-2000-101, *Submitted to Phys. Lett. B.*

[21] OPAL Collaboration, K. Ackerstaff *et al.* Eur. Phys. J. **C1** (1998) 395.

[22] D0 Collaboration, B. Abbott *et al.,* Phys. Rev Lett. **80** (1998) 3008;
CDF Collaboration, F Abe *et al.,* Phys. Rev Lett. **75** (1995) 11.

[23] J. Allison *et al.,* Nucl. Instr. Meth. **A317** (1992) 47.

[24] F. A. Berends *et al.*, Comput. Phys. Commun. **85**, (1995) 437.

[25] J. Fujimoto *et al.*, Comp. Phys. Commun. **100** (1997) 128.

[26] G. Marchesini *et al.,* Comp. Phys Commun. **67** (1992) 465.

[27] T. Sjöstrand, Comp. Phys Commun. **82** (1994) 74.

[28] M. Skrzypek *et al.,* Comp. Phys Commun. **94** (1996) 216;
M. Skrzypek *et al.,* Phys. Lett **B372** (1996) 289.

[29] R. Engel, Z. Phys. **C66** (1995) 203;
R. Engel, J. Ranft, and S. Roesler, Phys. Rev. **D52** (1995) 1459;
R. Engel and J. Ranft, Phys. Rev. **D54** (1996) 4244.

Fit	$\tilde{\kappa}_{\mathrm{z}}$	g_4^{z}	$\tilde{\lambda}_{\mathrm{z}}$
SDM Elements	$-0.19^{+0.08}_{-0.07}$	$0.00^{+0.21}_{-0.20}$	$-0.12^{+0.17}_{-0.16}$
$\cos\theta_{\mathrm{W}}$	$-0.19^{+0.46}_{-0.08}$	$0.7^{+0.4}_{-1.8}$	$-0.29^{+0.69}_{-0.11}$
Combined	$-0.19^{+0.06}_{-0.05}$	$0.01^{+0.22}_{-0.22}$	$-0.19^{+0.18}_{-0.13}$
Expected Stat. Error	± 0.11	± 0.19	± 0.12
Final Fit Including Systematics	$-0.20^{+0.10}_{-0.07}$	$-0.02^{+0.32}_{-0.33}$	$-0.18^{+0.24}_{-0.16}$

Table 3: Measured values of the CP-violating TGC parameters. Both the SDM elements for the leptonically decaying W and the $\cos\theta_{\mathrm{W}}$ production distribution in $\mathrm{qq}\ell\nu$ events from the 189 GeV data are used in the calculation. Errors are statistical only except in the case of the final combined fit.

Systematic	TT	LL	TL	T,L
Jet Reconstruction				
WW$\rightarrow$ qq$\ell\nu$	0.013	0.004	0.008	0.007
W$\rightarrow$ $\ell\nu$	-	-	-	0.005
W$\rightarrow$ qq	-	-	-	0.011
Hadronisatation				
WW$\rightarrow$ qq$\ell\nu$	0.016	0.002	0.014	0.009
W$\rightarrow$ $\ell\nu$	-	-	-	0.003
W$\rightarrow$ qq	-	-	-	0.021
MC Generator				
WW$\rightarrow$ qq$\ell\nu$	0.015	0.013	0.028	0.001
W$\rightarrow$ $\ell\nu$	-	-	-	0.004
W$\rightarrow$ qq	-	-	-	0.006
Background				
WW$\rightarrow$ qq$\ell\nu$	0.004	0.001	0.004	0.002
W$\rightarrow$ $\ell\nu$	-	-	-	0.003
W$\rightarrow$ qq	-	-	-	0.004
Lepton id				
WW$\rightarrow$ qq$\ell\nu$	0.017	0.005	0.014	0.010
W$\rightarrow$ $\ell\nu$	-	-	-	0.017
W$\rightarrow$ qq	-	-	-	0.003
Detector Effect Correction				
WW$\rightarrow$ qq$\ell\nu$	0.004	0.008	0.012	0.002
W$\rightarrow$ $\ell\nu$	-	-	-	0.009
W$\rightarrow$ qq	-	-	-	0.005
Charge Misassignment				
WW$\rightarrow$ qq$\ell\nu$	0.007	0.001	0.008	0.005
W$\rightarrow$ $\ell\nu$	-	-	-	0.011
W$\rightarrow$ qq	-	-	-	0.001
Total				
WW$\rightarrow$ qq$\ell\nu$	0.032	0.017	0.038	0.016
W$\rightarrow$ $\ell\nu$	-	-	-	0.023
W$\rightarrow$ qq	-	-	-	0.025

Table 4: The contribution to the systematic uncertainty on the polarised cross-section fractions from different sources.

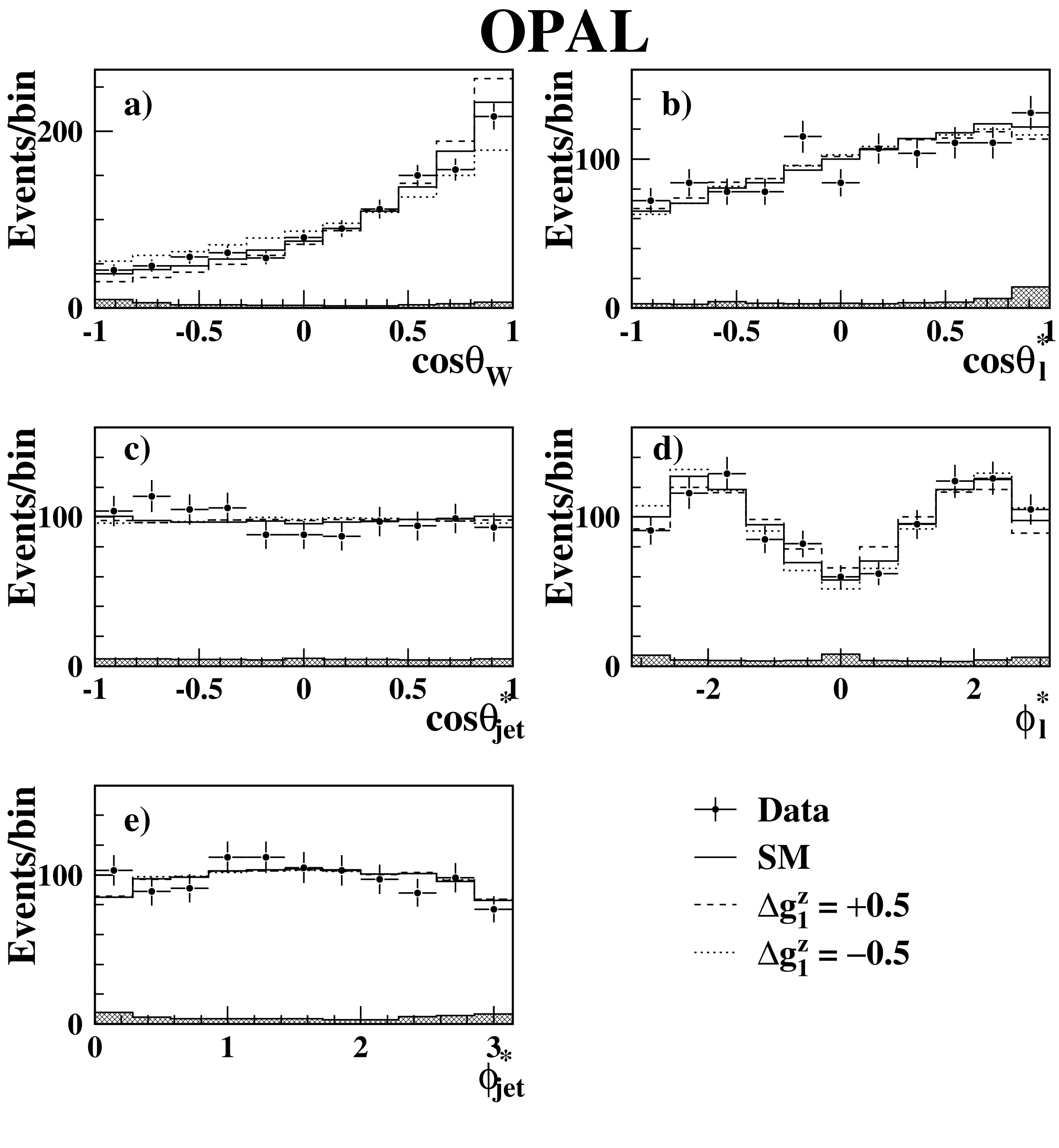

Figure 1: Distributions of the kinematic variables $\cos\theta_{\mathrm{W}}$, $\cos\theta^*_l$, $\cos\theta^*_{\mathrm{jet}}$, ϕ^*_l and ϕ^*_{jet}, as obtained from the qq$\ell\nu$ events. The points represent the data. The histograms show the expectation of the Standard Model and the cases $\Delta g_1^z = \pm 0.5$. The shaded histogram shows the non-qq$\ell\nu$ background. In the case of the W^+ decaying to the lepton, the value of ϕ^*_l is shifted by π in order to overlay the W^+ and W^- distributions.

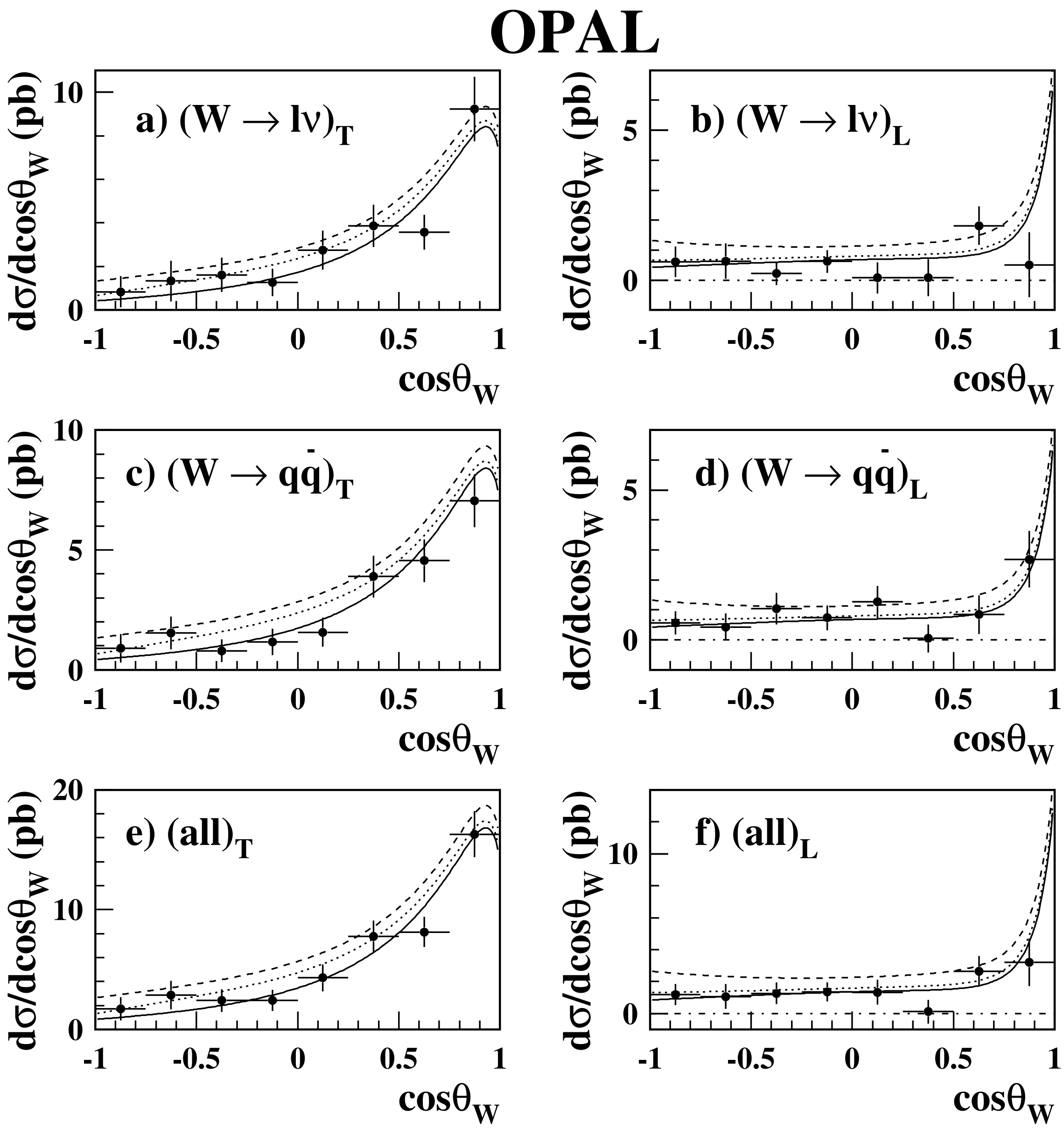

Figure 2: The polarised differential W production cross-sections. a) is the differential cross-section for transversely polarised leptonically decaying W bosons in the W boson pair and b) is for longitudinally polarised. c) and d) are as a) and b) but are shown for the hadronically decaying W boson in the pair. e) and f) are the combinations of the leptonically and hadronically decaying W. Overlaid are the predictions for the Standard Model (solid line) and CP-violating anomalous couplings $\tilde{\lambda}_z = -0.5$ (dotted line), $\tilde{\kappa}_z = +0.5$ (dashed line). The dotted-dashed line in b) and f) shows the zero. The errors include both statistical and systematic uncertainties.

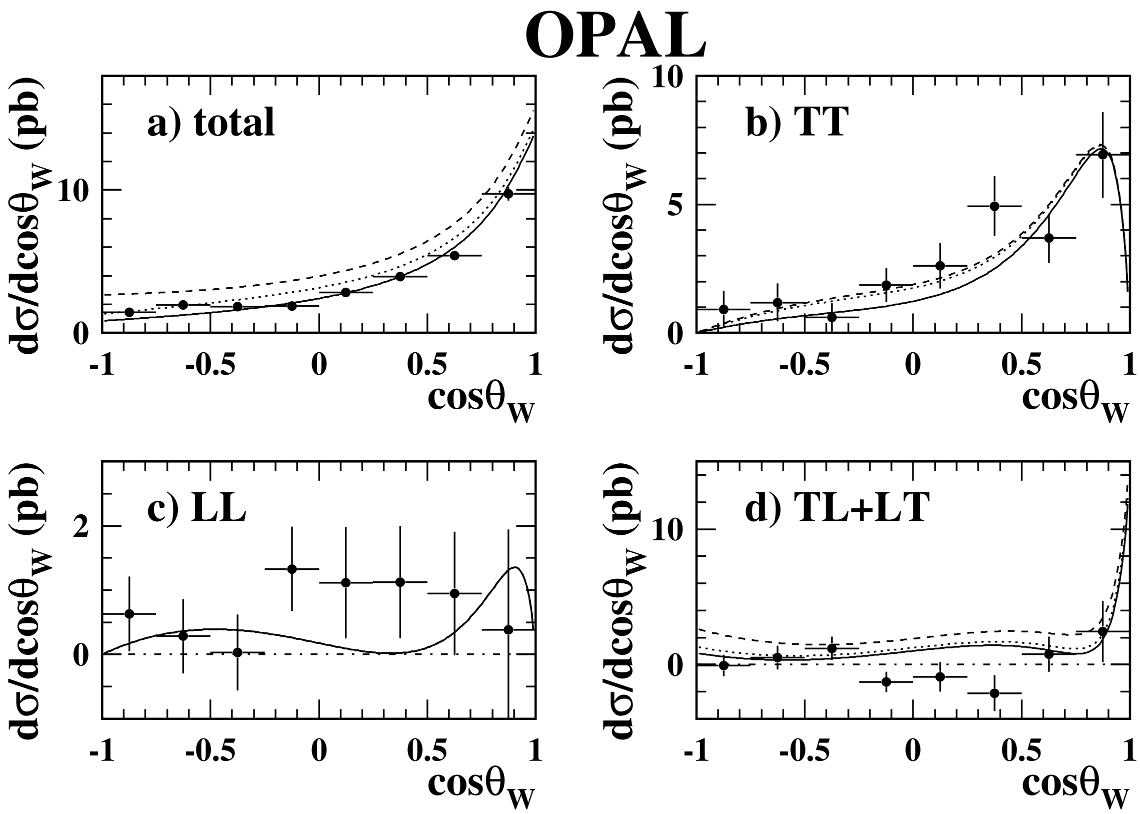

Figure 3: The differential cross-sections for the W bosons of different helicity states. a) is the corrected total W production differential cross-section, b) is for production of pairs of transversely polarised W bosons, c) is pairs of longitudinally polarised W bosons and d) is for one of each. Overlaid are the predictions for the Standard Model (solid line) and CP-violating anomalous couplings $\tilde{\lambda}_z = -0.5$ (dotted line), $\tilde{\kappa}_z = +0.5$ (dashed line). Only the solid line is visible on plot c) because this distribution is insensitive to the CP-violating couplings. The dotted-dashed line on plots c) and d) shows the zero. The errors include both statistical and systematic uncertainties.

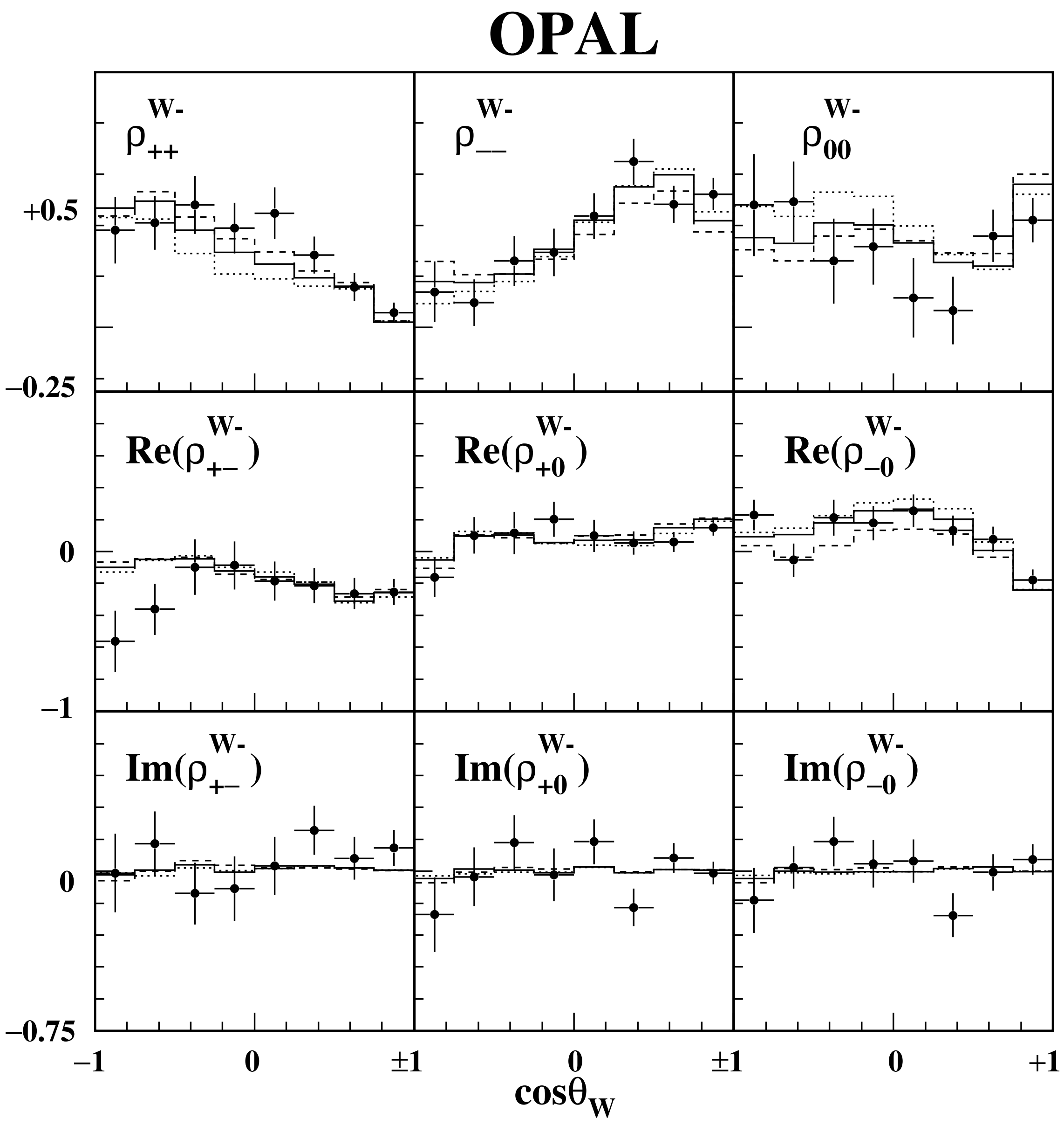

Figure 4: The individual W SDM elements extracted from the leptonically decaying W boson in the qq$\ell\nu$ data events at 189 GeV. The points are the OPAL data . The histograms represent the Monte Carlo predictions calculated from fully detector simulated Monte Carlo. The solid line shows the Standard Model expectation and the dotted (dashed) line that for $\Delta g_1^z = +0.5$ (-0.5). CPT invariance has been assumed in calculating these elements. The errors are both statistical and systematic.

OPAL

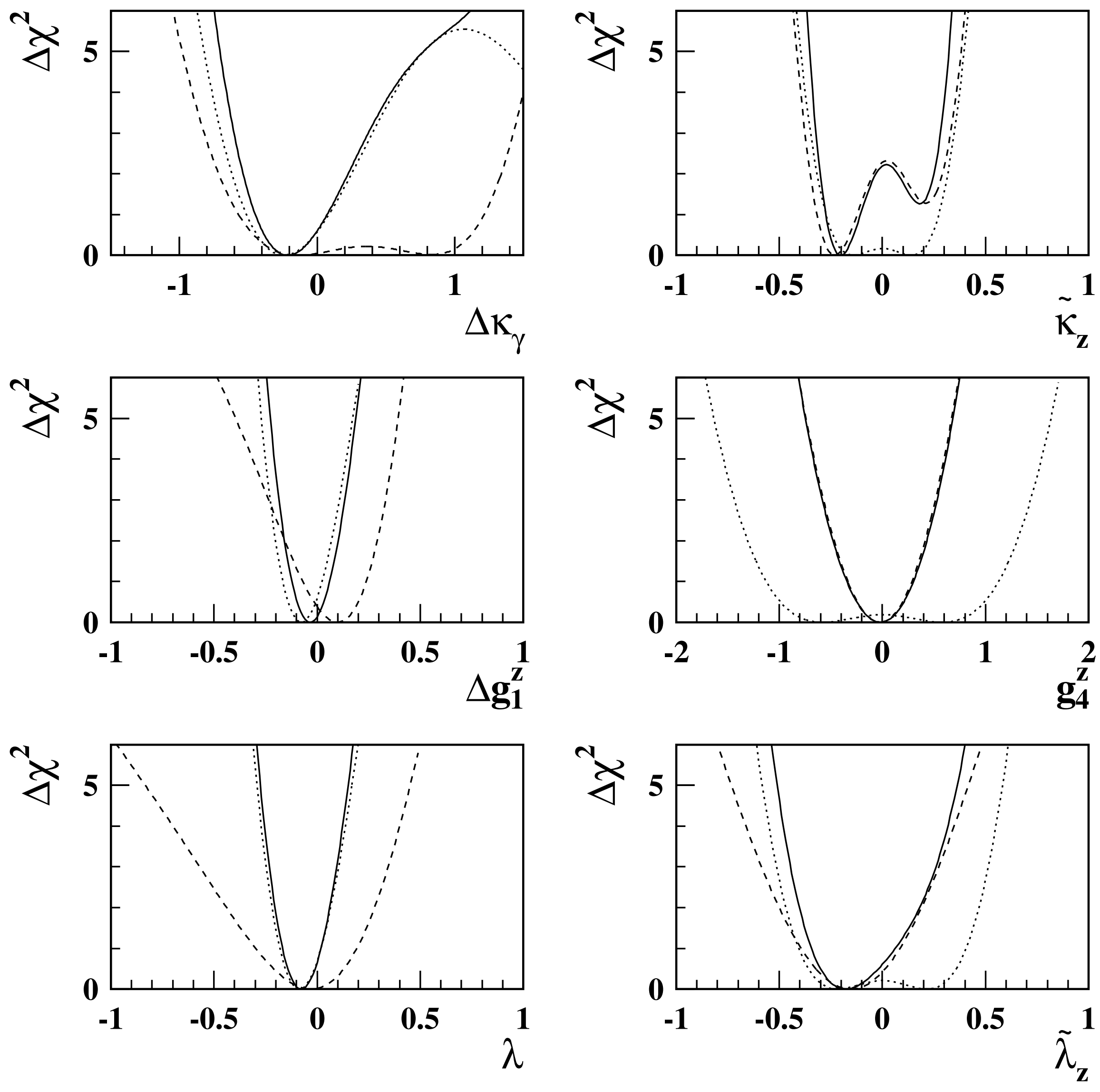

Figure 5: The χ^2 plots for the fits to the CP-conserving and CP-violating anomalous couplings. For the CP-conserving couplings the dashed line is the fit to just the 6 real SDM elements, for the CP-violating couplings it is the fit to all 9 SDM elements. The dotted line is the fit to just the $\cos\theta_W$ distribution. The solid line is the combined fit. All fits include systematic uncertainties.

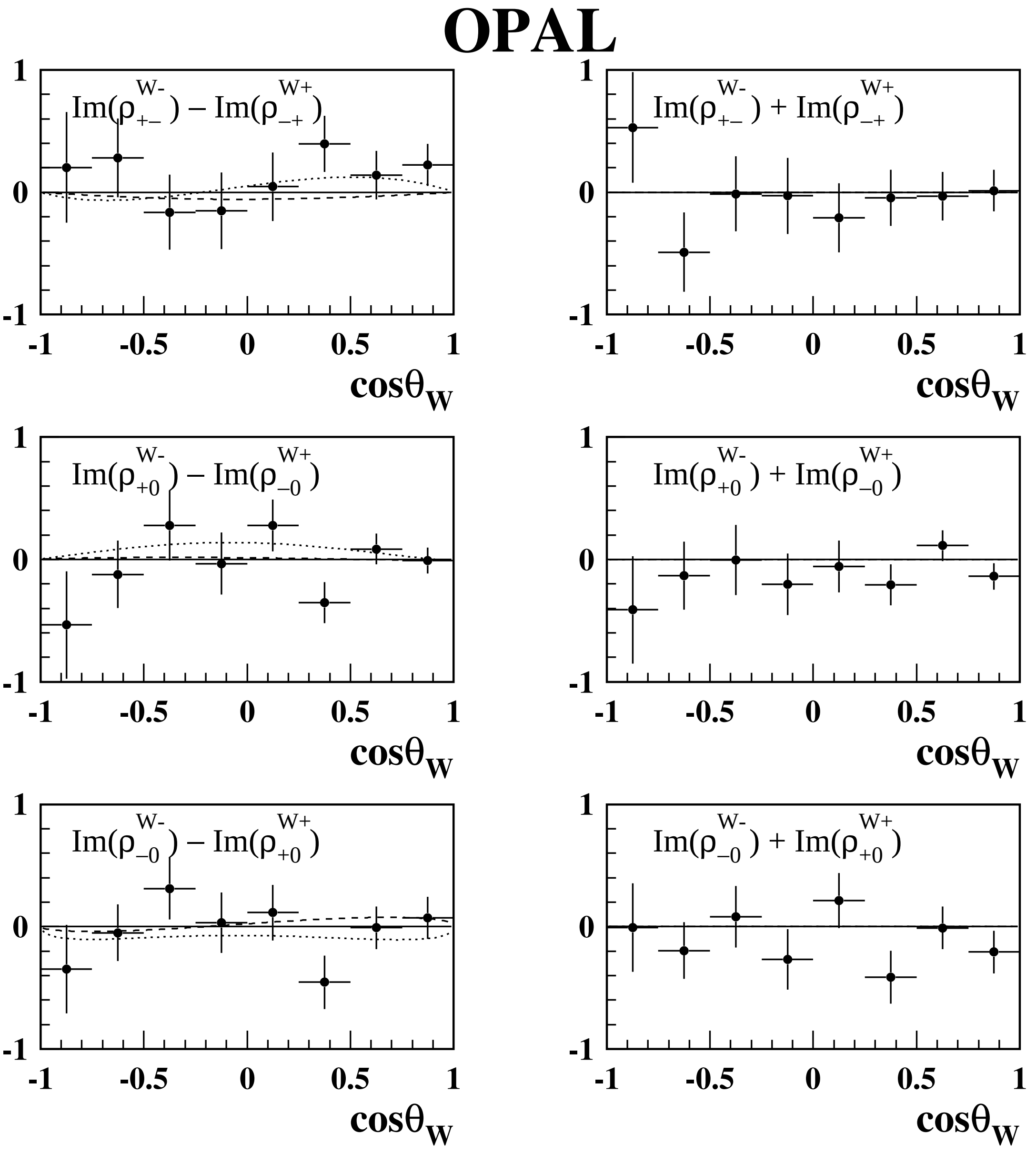

Figure 6: The combination of imaginary SDM coefficients sensitive to CP-violation at the triple gauge boson vertex for the 189 GeV data (three left side plots). Overlaid are the Born level predictions for the Standard Model (solid line) and also anomalous CP-violating couplings $\tilde{\lambda}_z = -0.5$ (dotted line) and $\tilde{\kappa}_z = +0.5$ (dashed line). Also shown are the combination of imaginary SDM coefficients sensitive only to loop effects (any deviation from zero) from the 189 GeV data (three right side plots). In all cases the errors include both statistical and systematic uncertainties.